
Improving Adversarial Robustness Through Progressive Hardening

Chawin Sitawarin *
UC Berkeley
chawins@eecs.berkeley.edu

Supriyo Chakraborty
IBM T. J. Watson Research Center
supriyo@us.ibm.com

David Wagner
UC Berkeley
daw@cs.berkeley.edu

Abstract

Adversarial training (AT) has become a popular choice for training robust networks. However, by virtue of its formulation, AT tends to sacrifice clean accuracy heavily in favor of robustness. Furthermore, AT with a large perturbation budget can cause models to get stuck at poor local minima and behave like a constant function, always predicting the same class. To address the above concerns we propose Adversarial Training with Early Stopping (ATES). The design of ATES is guided by principles from curriculum learning that emphasizes on starting “easy” and gradually ramping up on the “difficulty” of training. We do so by early stopping the adversarial example generation step in AT, progressively increasing difficulty of the samples the network trains on. This stabilizes network training even for large perturbation budgets and allows the network to operate at a better clean accuracy versus robustness trade-off curve compared to AT. Functionally, this leads to a significant improvement in both clean accuracy and robustness for ATES models.

1 Introduction

Deep neural networks have been shown to be vulnerable to carefully crafted adversarial examples [1, 2, 3]. When coupled with the increase in adoption of deep learning for mission critical tasks (e.g., identity verification, malware detection, self-driving vehicles) these vulnerabilities raise serious concerns. Understandably, robustness against such attacks is a desirable property for any network and several defenses have been proposed towards this end. While some of these defenses have been broken using newer and more sophisticated attacks, few have shown better resilience [4]. The one that has been the most successful and widely used is adversarial training (AT) [5]. Formulated as a minimax problem, AT essentially trains a network (outer minimization) on adversarial examples generated from the training set (inner maximization) for a given perturbation budget.

Motivating Problems: While serving as a strong baseline, AT tends to sacrifice accuracy on benign or clean samples (clean accuracy) to gain accuracy on adversarial examples (adversarial accuracy). While this tradeoff between clean and adversarial accuracy is inevitable [6], AT seems to operate at points far from the best possible trade-off curve. Specifically, we identified two problems when using AT with standard benchmarking datasets. First, when training a model on MNIST with a large perturbation budget (≥ 0.35), we found that the model consistently gets stuck in a poor local minima. It behaves like a constant function and predicts the entire input space as a single class (Figure 1a: solid black line). Similar effect is also observed while training a ConvNet model on CIFAR-10 with a

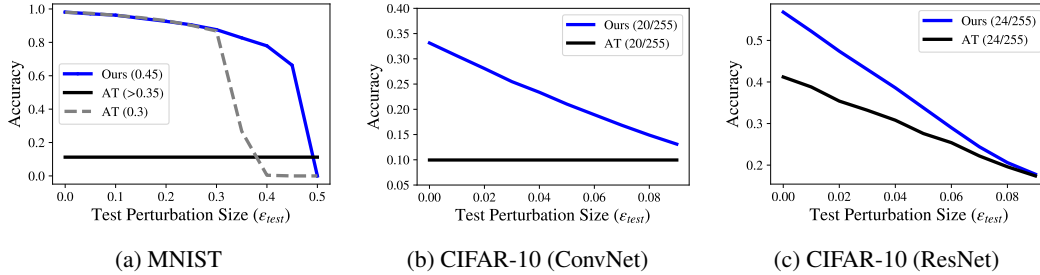


Figure 1: (a) and (b) illustrate a problem with AT (black lines), on MNIST and CIFAR-10 respectively, where models can get stuck at a trivial solution (i.e. a constant function) when trained with a large perturbation budget. Our approach (blue lines) reliably makes the exact same models trainable in these settings. (c) shows that AT can also result in a model with low clean accuracy which can be significantly improved by our method.

perturbation budget ($\geq 20/255$) (Figure 1b: solid black line). We then increased the model capacity, as suggested by the original AT paper, for both the datasets and found that the respective data models were able to train for larger perturbation budget, but they quickly get stuck again once the perturbation budget is further increased. Second, even when the training is not stuck, the models suffer from low clean accuracy (Figure 1c: solid black line achieves only 40% accuracy on clean data). Our goal is to develop a training strategy to solve both these problems simultaneously.

Connection to Curriculum Learning: We posit that both problems stem from the model being presented with adversarial examples that are “too difficult to learn from” at the beginning of the training process. This leads the model to be “overly pessimistic” and overcompensate by either (1) behaving like a constant function so that samples from at least one class are classified correctly; or (2) by construction focusing solely on the perturbed samples and hence, sacrificing clean accuracy. We observe that the concept of curriculum learning [7], which suggests that a model should learn from the “easy” samples first before being introduced to the “hard” ones naturally addresses these issues. However, one of the main criticism of curriculum learning is that the notion of “difficulty” of samples is not well-defined and hard to measure. Luckily, in the AT framework, there exists a set of parameters which can be readily used as a difficulty metric to dictate a curriculum. In fact, prior works have used perturbation budget [8] and *convergence scores* [9] as difficulty metrics with AT.

Contributions: In this work, we propose Adversarial Training with Early Stopping (ATES), to significantly improve clean accuracy and achieve at least comparable adversarial accuracy at any perturbation budget compared to AT. In other words, our approach reaches a better trade-off curve than AT by improving both model robustness and clean accuracy simultaneously. Inspired by curriculum learning, we define a *softmax probability gap* as a difficulty metric. We then use early stopping on the adversarial example generation step to control this probability gap and generate a curriculum during training. Our scheme stabilizes the early stage of the training and yield models that have higher accuracy and comparable or higher robustness than AT.

We validate our scheme by performing a systematic evaluation against multiple datasets (MNIST, CIFAR-10, CIFAR-100). Highlights of the results include: ATES allows the MNIST model to train with perturbation budget of up to 0.45 (compared to 0.3 with AT) while still maintaining high accuracy on clean and adversarial data (Figure 1a: blue line). It also results in CIFAR-10 models that have comparable adversarial accuracy to AT at large perturbation but much higher accuracy at smaller or perturbation (Figure 1b, 1c: blue line). On ResNet-20, the clean accuracy improves from 42% to 57% when a perturbation budget of 24/255 is used, and with the budget of 8/255, we increase the clean accuracy from 82% to 87% and the adversarial accuracy from 44% to 49%.

2 Background

2.1 Adversarial Examples and Adversarial Training

Adversarial examples are a type of evasion attack against machine learning models generated by adding small perturbations to clean samples [2, 3]. The desired perturbation, constrained to be within some ℓ_p -norm ball around the clean sample, is typically formulated as a solution to the following

optimization problem:

$$x^{adv} = x + \delta^* \quad \text{where } \delta^* = \arg \max_{\delta: \|\delta\| \leq \epsilon_{\text{train}}} L(x + \delta) \quad (1)$$

where L is the loss function used by the target neural network. The ℓ_p -norm ball, bounded by the training perturbation budget, ϵ_{train} , is usually treated as a proxy for imperceptibility of the added perturbation. Projected gradient descent (PGD) [5] is a popular technique used to solve Eqn. (1). In a nutshell, the adversarial training (AT) algorithm, iteratively generates adversarial examples from every batch of the training data by solving Eqn. (1) and then trains a model on these examples. AT is formulated as an optimization of the saddle point problem as follows:

$$\arg \min_{\theta} \frac{1}{n} \sum_{i=1}^n \max_{\delta_i: \|\delta_i\| \leq \epsilon_{\text{train}}} L(x_i + \delta_i; \theta) \quad (2)$$

where θ are the model parameters, and $\{(x_i, y_i)\}_{i=1}^n$ denotes the training set. The inner maximization is typically solved using PGD, and the outer minimization (i.e. the training part) can be solved by mini batch SGD or by any other technique used for training deep neural networks.

2.2 Curriculum Learning

In Curriculum learning (CL) the main idea is to incorporate domain knowledge, from a “teacher,” to manipulate the sequence of training samples presented to the model or “student.” The sequence of samples introduced in non-decreasing order of some “difficulty” score, allows the student model to learn better. Since then, the concept has appeared in many influential works, especially related to unsupervised and semi-supervised learning, in computer vision [10, 11, 12], natural language processing [13, 14], and deep reinforcement learning [15, 16]. Theoretical aspects of CL using various difficulty metrics have been studied in [17].

3 Adversarial Training with Early Stopping

As previously mentioned, “starting off easy” is the key idea that we believe will address the two issues of poor local solutions and low clean accuracy. To this end, we rely on curriculum learning to provide the easy start necessary to both avoiding poor local minima and directing training towards more favorable regions to improve the final performance. In fact, it has been both theoretically (for a linear regression) and empirically established that presenting easier samples at the beginning of curriculum-based training improves the early convergence rate as well as the final generalization performance, especially when the task is difficult (e.g., under parameterized network, heavy regularization) [17].

3.1 Defining a Difficulty Metric

To create a curriculum, we need a difficulty metric for the training samples. We started by exploring a few intuitive strategies. For instance, to train an MNIST model with $\epsilon_{\text{train}} = 0.45$, we pre-trained a model with a small ϵ_{train} (or by using a small number of PGD steps) and then increased ϵ_{train} or simply scaled it linearly with the epoch number. Regardless, the training always converged back to the poor trivial solution after a certain number of epochs.

We notice that the gradients of the parameters have a very large norm and variance when trained on AT. This can be partially mitigated by using a small ϵ_{train} but not completely because the loss space near some sample may be very sensitive and a small perturbation can cause a large increase in loss which results in a very gradient updates on the parameters (see Appendix for more details). For this reason, we propose *softmax probability gap* as a difficulty metric to directly control the maximum loss a sample can incur.

For a given input sample, we define the probability gap as the difference between the largest softmax probability among any class excluding the correct one and the softmax probability of the correct class. Formally, the probability gap $g(x; \theta)$ is defined as:

$$g(x; \theta) := \max_{j \neq y} f(x; \theta)_j - f(x; \theta)_y \quad (3)$$

where (x, y) is a pair of input and its ground truth label, $f(\cdot; \theta)$ is the softmax output of a neural network parameterized by θ . For the rest of the paper, when θ is clear from the context, we will

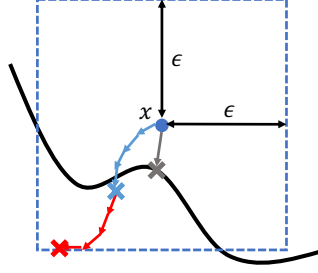


Figure 2: Comparison between the perturbed samples generated by AT and ATES. The gray cross is the adversarial example closest to the sample (blue dot) which is the ideal point to locate, but it is also prohibitively expensive to compute. The blue and red arrows represents PGD updates that perturb the sample towards the boundary. For ATES, the process stops once the boundary is crossed (blue cross), approximating the gray cross. But AT continues the update until a specified maximum step (red arrows and cross).

write $g(x; \theta)$ as $g(x)$ and $f(x; \theta)$ as $f(x)$. When $g(x) < 0$, x is correctly classified as class y . When $g(x) > 0$, x is misclassified, and when $g(x) = 0$, x is on the decision boundary between at least two classes.

Using this metric, we were not only able to train an MNIST model using $\epsilon_{\text{train}} = 0.45$ but also improve both clean and adversarial accuracy compared to AT at $\epsilon_{\text{train}} = 0.3$. The probability gap takes value in $[0, 1]$ which greatly simplifies its scheduling during training. It also requires no additional computation during training, and as we later show, it correlates with the other difficulty metrics suggested in prior works.

3.2 Our Approach

Our scheme, ATES, modifies the inner maximization of AT so that it only finds adversarial examples that are approximately on the boundary or $g(x + \delta) = 0$. In the form of optimization problem, ATES can be described as:

$$\arg \min_{\theta} \frac{1}{n} \sum_{i=1}^n \max_{\delta_i: \|\delta_i\| \leq \min\{\epsilon, d(x_i, \theta)\}} L(x_i + \delta_i; \theta) \quad (4)$$

where $d(x_i, \theta)$ defines the shortest distance from x_i to the decision boundary of class y_i . Note that $\epsilon(x_i, \theta) = \min\{\epsilon, d(x_i, \theta)\}$ is a function of x_i and the current model parameters θ which defines the boundary, similarly to the other adaptive methods. If $d(x_i, \theta) < \epsilon$, and the inner maximization does solve fully, then as desired, the inner optimizer will find an adversarial example that is right on the boundary; but if an adversarial example does not exist within the ϵ -ball, or $d(x_i, \theta) \geq \epsilon$, the inner optimization is equivalent to that of AT.

However, in practice, computing $d(x_i, \theta)$ is not feasible, and there is no guarantee that the inner maximization is solved fully. We propose a simple method to approximate the same effect by terminating the inner maximization as soon as the perturbed sample passes the boundary to the side of an incorrect class. At every PGD step, the output label is checked for match with the ground truth. If it does not, we ensure no additional perturbation is added to the sample. The perturbed samples will not be exactly on the boundary and likely use a larger perturbation than $d(x_i, \theta)$ (if $d(x_i, \theta) < \epsilon$), but the advantage is that it incurs a very small cost compared to computing $d(x_i, \theta)$. Figure 2 illustrates this process and conceptually compares ATES to AT.

ATES by default requires no additional parameter and creates an *implicit* form of curriculum when ensuring that $g(x + \delta) = 0$. The intuition here is that at the beginning, model’s predictions are mostly incorrect so a few correct samples are only pushed slightly to cross the boundary. This is when the generated adversarial examples that the model trains on are “easy.” After some updates the model adjusts its boundary so that more samples are on the correct side as well as to increase the margin. In the next iteration, the same set of training samples now must be pushed further to cross the boundary. As this process keeps repeating, the margins extend slowly, and the model becomes more robust. Thus, the adversarial examples at this later stage require larger perturbation and are considered “harder.”

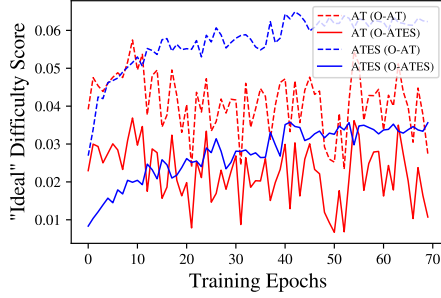


Figure 3: “Ideal” difficulty score of adversarial examples generated by AT (red) and ATES (blue) with respect to two oracles, O-AT (dashed), and O-ATES (solid). Only the ATES model shows a clear upwards trend on both oracles.

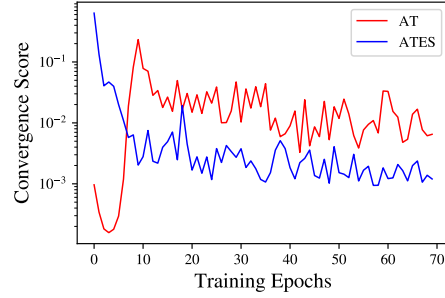


Figure 4: Median convergence score of AT (red) and ATES (blue). The ATES model starts from a large score and decreases consistently. The score is also an order of magnitude lower than AT, suggesting a good convergence quality.

3.3 Correlations with Other Difficulty Metrics.

We show correlation between probability gap and the difficulty metrics suggested in prior works. Hence, ATES also follows a similar curriculum and thus shares all its properties and benefits.

3.3.1 Ideal difficulty score.

The ideal difficulty score is defined as the loss of a given input according to the *optimal hypothesis* [17], or in this case, $L(x; \theta^*)$ for θ^* is the solution of Eqn. (2). It is suggested that the start of training be dominated by easy samples or samples with a low difficulty score, and then the samples become increasingly hard [7, 17]. To approximate the optimal hypothesis, we use two fully trained models as oracles, O-AT and O-ATES, which use a different architecture and random seed than AT and ATES. Figure 3 shows the average loss computed on each of the oracles using adversarial examples generated throughout the training of AT and ATES models. The scores of training samples in AT vary in a wide range and do not have clear trends. Conversely, for ATES, the training samples start off with a low score, and their score consistently increases throughout the training, indicating a steady increase in difficulty level.

3.3.2 Convergence score.

The convergence score is proposed as a metric to quantify the strength of an adversary or how well the inner maximization is solved [9]. To improve AT, the authors suggest that a high score is maintained at the beginning of training and then slowly decreased. They experimentally show that this form of curriculum increases the convergence quality of the adversarial examples in the later epochs, and training on these samples improves the final robustness.

The convergence score measures the the Frank-Wolfe gap of the inner maximization which is zero when it is solved completely. It is defined as follows:

$$c(x + \delta) = \epsilon \|\nabla_{\mathbf{x}} L(x + \delta; \theta)\|_1 - \langle \delta, \nabla_{\mathbf{x}} L(x + \delta; \theta) \rangle \quad (5)$$

Figure 4 compares progression of the convergence score between AT and ATES on MNIST (note the log scale). Notice that median of the convergence score of ATES starts off at the highest point and consistently goes down, but for AT, the score is initially very small. Then it shoots up high and only slowly decreases as training progresses. Additionally, ATES also reaches a much lower score than AT, suggesting that it finds adversarial examples with better convergence quality. This result indicates that our scheme does follow the framework recommended by [9], and hence, it should receive similar benefits.

3.4 Augmenting ATES

Below we describe ways to further improve the performance of ATES introducing an explicit control parameter γ and by using a cyclical learning rate schedule.

3.4.1 Using Explicit Control

ATES can be generalized by introducing a parameter that controls the early stopping criterion when $g(x + \delta) = \gamma$ for some $\gamma \geq 0$. Fixing γ at 0 throughout the training yields ATES, and setting $\gamma \geq 1$ is equivalent to AT. Increasing γ as training progresses provides an explicit form of curriculum. In this sense, ATES can be viewed as the “weakest” adversary and AT as the “strongest.” In our experiments on CIFAR-10, we will use this explicit schedule by increasing γ in steps of 0.333 for three times. We call this scheme ATES-S. We find that increasing γ at the same epoch the learning rate is reduced generally performs well.

3.4.2 Using Cyclic Learning Rate

We also observed that cyclical learning rate [18, 19] further improves the performance of both ATES and AT. The same observation has also made in [20]. We use the one-cycle learning rate when training models on CIFAR-10 for 100 epochs. We initialize the learning rate to a small value and then linearly increase it after every step. The learning rate reaches the maximal value around epoch 50 and then we linearly reduce the learning rate such that the minimal value is attained by the end of the training.

Interestingly, the authors in [19] mention that cyclical learning rate is inspired by curriculum learning and simulates annealing. Since it does not order the training samples according to some metric, cyclical learning rate does not follow the definition of a curriculum as defined by [17]. Nonetheless, it provides similar benefits that also helps address the two problems we identified with AT. The slow start seems to prevent overcompensation in the early epochs and the larger learning rate later on encourages more exploration, resulting in a model with better clean and adversarial accuracy.

4 Experiments

4.1 Setup

In this section, we test the robustness of AT and ATES models on three image datasets, namely MNIST, CIFAR-10, and CIFAR-100. We use PGD with random restarts for evaluating the robustness, where \mathcal{S} -PGD denotes PGD with \mathcal{S} steps. Additionally, since adversarial robustness evaluation is notoriously difficult, we strengthen ours by using our improved version of PGD, named PGD+, which leverages better initialization and loss functions. See Appendix for details.

4.1.1 MNIST.

All experiments use the same three-layer convolution network. Models are trained for 70 epochs. The initial learning rate is set at 0.01 and is decreased by a factor of 10 at epochs 40, 50, and 60. During training, we run PGD for 40 steps with a step size of 0.02 and use a uniform random initialization within the ℓ_∞ -ball of radius ϵ_{train} for both AT and ATES.

4.1.2 CIFAR-10/CIFAR-100.

We use both pre-activation ResNet-20 [21] and WideResNet-34-10 [22], which are trained for 100 epochs. Both AT and ATES use PGD with 10 steps and random restart. For $\epsilon_{\text{train}} < 16/255$, we use an initial learning rate of 0.1 and PGD step size of $2/255$. Otherwise, the initial learning is reduced to 0.01 with PGD step size of $4/255$. Standard data augmentation (random crop, flip, scaling, and brightness jitter) is also used.

4.2 Results on MNIST

In Figure 5, we compare the robustness of ATES to AT on MNIST for a range of ϵ_{test} values. We train four models with ATES using $\epsilon_{\text{train}} = 0.3, 0.35, 0.4$, and 0.45 , but we could not use AT to train models using $\epsilon_{\text{train}} \geq 0.35$. Based on the experiments we make several observations below.

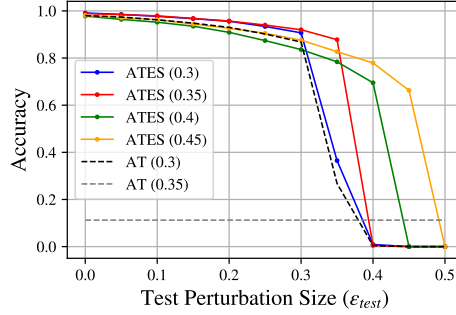


Figure 5: (MNIST) Adversarial accuracy vs. the perturbation norm (ϵ_{test}) for AT and ATEs trained under various values of ϵ_{train} , indicated by the numbers in parentheses. Note that this plot uses the strong but expensive PGD+ to calculate adversarial accuracy. Hence, we can only evaluate on the first 1,000 test samples.

Networks	No Attack	20-PGD	100-PGD	500-PGD	PGD+
AT ($\epsilon_{\text{train}} = 0.3$)	0.9799	0.8904	0.8867	0.8856	0.8730
ATES ($\epsilon_{\text{train}} = 0.3$)	0.9916	0.9308	0.9267	0.9275	0.9218
ATES ($\epsilon_{\text{train}} = 0.35$)	0.9911	0.9404	0.9382	0.9366	0.9309
ATES ($\epsilon_{\text{train}} = 0.4$)	0.9823	0.8954	0.8934	0.8947	0.8716
ATES ($\epsilon_{\text{train}} = 0.45$)	0.9835	0.9227	0.9194	0.9184	0.9003

Table 1: (MNIST) Accuracy of our scheme ATEs compared to AT under no attack and different attacks at $\epsilon_{\text{test}} = 0.3$. Note that numbers in this table are computed on the entire test set.

4.2.1 ATEs avoids poor local minima when trained with large perturbation.

AT on MNIST with an ℓ_{∞} -norm perturbation usually fails when ϵ_{train} is larger than a certain value, which is 0.35 in our setting. The training “gets stuck” after a few iterations. The model becomes a constant function and outputs the same logits and class for every input (dotted gray line in Figure 5). Changing the optimizer or the initial learning rate can help in some cases, but doing so does not allow us to perform AT with any $\epsilon_{\text{train}} \geq 0.35$.

Since MNIST digits mostly take values very close to 0 and 1, the limiting perturbation of size 0.35, which is still lower than the expected robustness of close to 0.5, seems to be an artifact of the optimization rather than a natural limitation of the dataset or the model. We confirm this by training on $\epsilon_{\text{train}} > 0.3$ with ATEs using the same model, optimizer, and learning rate as AT. Figure 5 shows that all the models trained by our scheme do not get stuck and achieve considerably high adversarial accuracy at $\epsilon_{\text{test}} = \epsilon_{\text{train}}$.

4.2.2 ATEs is more robust and has higher clean accuracy.

Table 1 benchmarks accuracy of all five models at $\epsilon_{\text{test}} = 0.3$. They are evaluated by PGD with various number of steps as well as PGD+. In fact, this also confirms that our PGD+ reliably outperforms the original PGD on all of the models. ATEs with ϵ_{train} of 0.3 and 0.35 have slightly higher clean accuracy and significantly higher adversarial accuracy than AT at $\epsilon_{\text{train}} = 0.3$. This demonstrates two benefits of ATEs. First, it can achieve a point above the accuracy-robustness trade-off curve of AT. As generally observed, gaining more robustness at some ϵ usually sacrifices accuracy of the same model on clean samples. However, our scheme achieves higher accuracy than AT in both the normal and the adversarial settings. The second observation is ATEs with ϵ_{train} of 0.35 is even more robust than the one trained at $\epsilon_{\text{train}} 0.3$, suggesting that with our approach, training at a larger ϵ than the target one can provide an additional boost to robustness. We will also leverage this effect when training ATEs on CIFAR-10.

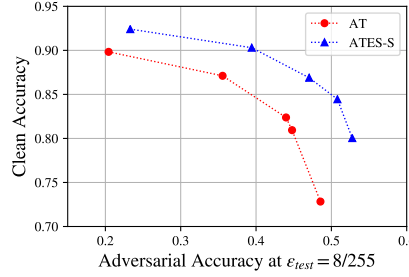


Figure 6: (CIFAR-10) The trade-off curve of ATES-S appears entirely above that of AT. Each point represents a model that is trained with either ATES-S or AT with ϵ_{train} of 2, 4, 6, 8, and 10 out of 255 from left to right.

4.2.3 No gradient obfuscation.

To confirm that the ATES models do not appear robust due to the obfuscated gradients [4], we experiment with two more recent attacks that claim to mitigate the gradient obfuscation problem: Sign-OPT [23] and Brendel & Bethge (BB) [24]. Sign-OPT only relies on hard labels output by the network and not on gradients or logits. BB still utilizes gradient information, but the attack is initialized from a point that is already misclassified and is claimed to reliably find minimum-norm adversarial examples.

We run both attacks on the first 100 test samples with their default parameters as well as some tuning.² In total, 19 adversarial examples are found by Sign-OPT and 10 by BB on ATES with $\epsilon_{train} = \epsilon_{test} = 0.45$. On the other hand, our PGD+ attack finds 30 adversarial examples in total which also contain all of the ones found by Sign-OPT and BB. This experiment suggests that PGD+ is a stronger attack than the other two and that the robustness of ATES is unlikely to come from obfuscated gradients.

4.2.4 Cyclical Learning rate does not prevent poor local minima but using a warm start from ATES does.

The poor local minima where AT models get stuck in for large ϵ_{train} cannot be avoided by using cyclical learning rate. This is expected since our experiments with different initial learning rates also fail to make any difference. On the contrary, this issue can be resolved when we start training a model with ATES then switch to AT only after a few epochs. This observation aligns with our intuition and emphasizes that curriculum learning stabilizes the optimization and directs it towards more favorable loss regions.

4.3 Results on CIFAR-10

Given a fixed ϵ_{test} , models trained on varied ϵ_{train} form an accuracy-robustness trade-off curve, illustrated in Figure 6. A robust training algorithm is only considered superior to another when its trade-off curve lies above the other’s curve. Our experiment shows that ATES-S (blue triangles) indeed achieves this and clearly reaches a better trade-off curve than AT (red dots).

4.3.1 ATES increases clean accuracy but lowers adversarial accuracy.

Figure 7a and 7b shows that ATES (blue) increases the clean accuracy by a large margin ($\approx 8\%$) but loses about 1% of the robust accuracy compared to AT trained at the same $\epsilon_{train} = 8/255$. In fact, this is expected because ATES is a *weaker* adversary as mentioned in Section 3.2. Another way to quantify the adversary’s strength is through the optimal value of the inner maximization. Since the feasible set of ATES is a subset of that of AT, the optimal loss of ATES cannot be larger than that of

²We have to run Sign-OPT as a targeted attack and try all incorrect labels since its untargeted version does not work as well. This increases the computation time significantly and limits the experiment to only 100 samples. Sign-OPT code is from https://github.com/cmhcbb/attackbox/blob/master/sign_sgd/OPT_attack_1f.py, and BB code is from Foolbox 3.0

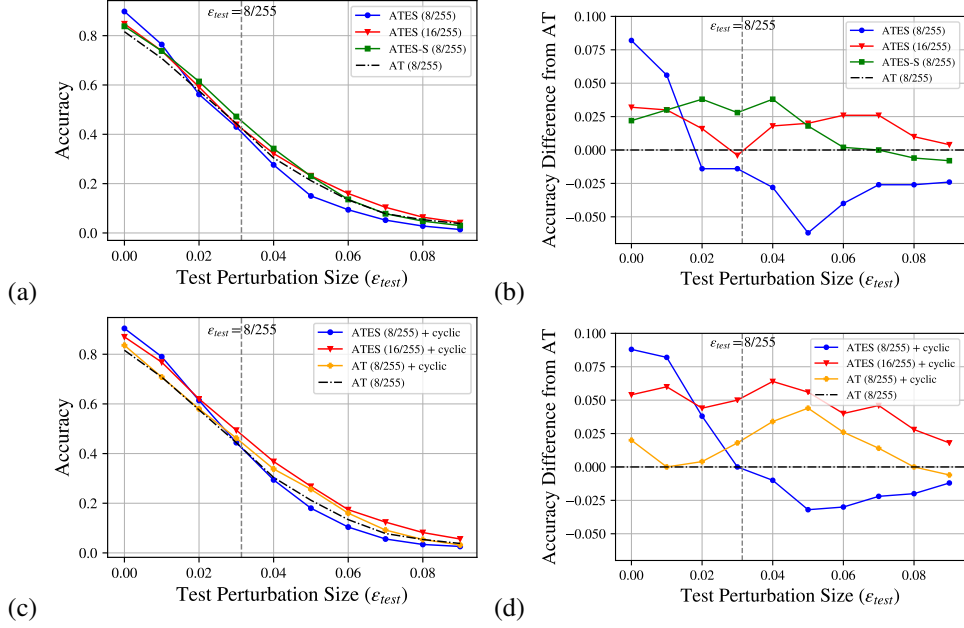


Figure 7: (CIFAR-10) **Top:** (a) accuracy and (b) accuracy difference between AT and ATEs trained using SGD with the default learning rate schedule, measured at a range of ϵ_{test} . **Bottom:** (c) and (d) are counterparts of (a) and (b) but compare AT to ATEs trained using SGD with the cyclical learning rate. The numbers in parentheses on the legends indicate ϵ_{train} .

AT, given the same θ . Consequently, it is possible that ATEs never sees the worst-case adversarial examples for some training samples, resulting in a drop on adversarial accuracy for larger ϵ_{test} .

4.3.2 ATEs-S improves both clean and adversarial accuracy.

Here, we experiment with two ways of increasing the strength of adversary for ATEs. First, we find that simply increasing ϵ_{train} from 8/255 to 16/255 (red curve in Figure 7a and 7b) does the trick. It increases adversarial accuracy from AT for the entire range of ϵ_{test} except for around 8/255. This option is simple and does not introduce scheduling, but it can be difficult to find an appropriate ϵ_{train} that provides a robustness boost at some $\epsilon_{\text{test}} < \epsilon_{\text{train}}$.

The second option uses the augmentation which explicitly controls γ , or ATEs-S. This scheme is represented by the green curve in Figure 7a and 7b. ATEs-S increases both clean and adversarial accuracy up to $\epsilon_{\text{test}} = 0.05$ compared to AT.

4.3.3 Cyclical learning rate further improves the performance.

Figure 7c and 7d demonstrate the performance improvement with the cyclical learning rate for all the models (AT, ATEs, and ATEs with larger perturbation) and for the entire range of ϵ_{test} compared to without. The ATEs model now has 9% higher clean accuracy compared to the original AT with the similar robust accuracy at $\epsilon_{\text{test}} = 8/255$. Additionally, the ATEs model with a larger $\epsilon_{\text{train}} = 16/255$ has 5% increase on both clean and adversarial accuracy compared to AT. It also has higher accuracy than AT at all ϵ_{test} , indicating that it does lie on a better trade-off curve than AT. The ATEs-S model with the cyclical learning rate (not shown) also improves in a similar manner but to a slightly smaller degree.

4.3.4 Bigger improvement with larger perturbation.

Our scheme can improve the performance of AT even more significantly when ϵ_{train} is large. This agrees with the observation made by [17] that curriculum learning contributes more when the task is more difficult. Figure 8 demonstrates a similar trend on networks trained with AT and ATEs-S at $\epsilon_{\text{train}} = 12/255, 16/255$, and $24/255$. ATEs-S models always improve clean accuracy by a large margin and simultaneously, increase the robustness at almost every ϵ_{test} . Again, cyclical learning rate

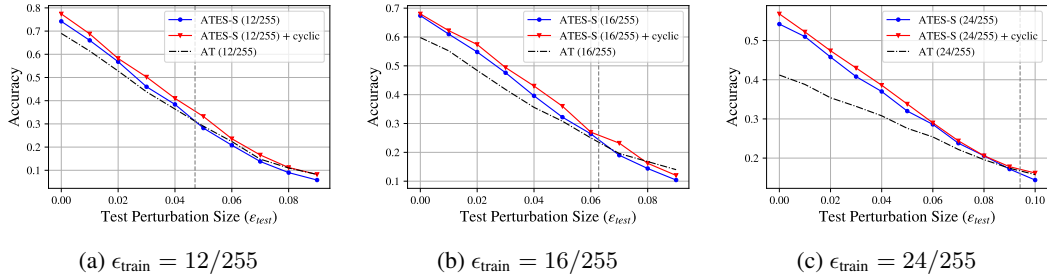


Figure 8: (CIFAR-10) Accuracy vs. ϵ_{test} plots comparing models trained with AT, ATES-S, and ATES-S with the cyclical learning rate. The gray dashed line denotes $\epsilon_{\text{test}} = \epsilon_{\text{train}}$ for each plot.

Networks	No Attack	20-PGD	100-PGD	PGD+
AT ($\epsilon_{\text{train}} = 8/255$)	0.8618	0.5329	0.5150	0.5027
ATES ($\epsilon_{\text{train}} = 16/255$)	0.8895	0.5284	0.5025	0.4869
ATES-S ($\epsilon_{\text{train}} = 8/255$)	0.8684	0.5506	0.5318	0.5131

Table 2: (CIFAR-10) Clean and adversarial accuracy at $\epsilon_{\text{test}} = 8/255$ of WideResNet-34-10 models.

consistently boosts the accuracy even further, but the overall improvement may diminish at a very large ϵ_{test} .

4.4 Benchmarking on CIFAR-10 and CIFAR-100

Here, we experiment with a common benchmarking model on CIFAR-10 and CIFAR-100, WideResNet-34-10, which contains more than 4 times the number of parameters of ResNet-20. On CIFAR-10 (Table 2), ATES-S again achieves higher accuracy both clean and adversarial than AT on all the attacks. The ATES with a larger perturbation size ($\epsilon_{\text{train}} = 16/255$) increases the clean accuracy but is less robust than AT. We also experiment with the cyclical learning rate, but it does not help improve the accuracy in this case. We suspect that the smaller improvement on WideResNet compared to on ResNet is due to the increase in capacity of the model. When model capacity is sufficiently large with respect to the task, i.e. the task becomes relatively easier, and effects of curriculum learning can become less prominent [17].

As shown in Table 3, the results on CIFAR-100 also have a similar trend as on CIFAR-10. Compared to AT, ATES-S improves the clean accuracy by over 2% while maintaining very slightly higher adversarial accuracy. The other difference from CIFAR-10 is that ATES-S also has higher clean accuracy than ATES with $\epsilon_{\text{train}} = 16/255$.

5 Related work

Several prior works have attempted to improve AT in terms of computation time, robustness gain, and clean accuracy. Some have tried different loss functions that are better suited to adversarial training [25, 26, 27]. This line of work is orthogonal to ours as we choose not to modify the loss function. Instead, we focus on improving both clean and adversarial accuracy on the adversarial example generation process and without incurring any additional computation cost.

Our approach also has similarities with a recent work in [8] and concurrent work in [28]. Both rely on using an adaptive perturbation for the training samples. In other words, the fixed perturbation budget, ϵ_{train} , in Eqn. (2) is now treated as a function of both the training sample x_i and the model parameter θ , i.e., $\epsilon_i = \epsilon(x_i, \theta)$. Their key insight is that some adversarial examples can be further or closer to the “ideal” decision boundary than that generated by using a fixed ϵ_{train} . Since there is no efficient way to compute the exact margin, in [8] the authors increase (or decrease) ϵ_i during training by a small amount every time the adversarial example generated within the given ϵ_i -ball is correctly (or incorrectly) classified. The authors in [28] take a similar approach, but in addition also perform label smoothing during training. In contrast, our approach focuses more on incorporating a curriculum into

Networks	No Attack	20-PGD	100-PGD	PGD+
AT ($\epsilon_{\text{train}} = 8/255$)	0.6077	0.2763	0.2645	0.2507
ATES ($\epsilon_{\text{train}} = 16/255$)	0.6193	0.2538	0.2381	0.2358
ATES-S ($\epsilon_{\text{train}} = 8/255$)	0.6295	0.2805	0.2656	0.2514

Table 3: (CIFAR-100) Clean and adversarial accuracy at $\epsilon_{\text{test}} = 8/255$ of WideResNet-34-10 models.

AT and by using early stopping in the inner maximization, our method implicitly uses an adaptive ϵ_i for all the training samples and does not require bookkeeping of ϵ_i for each training sample.

Curriculum learning has also been applied to improve adversarial robustness. In curriculum adversarial training [29], the authors create a curriculum by slowly increasing the values of ϵ_{train} during training. But their empirical results suggest that the curriculum alone is not effective and must be combined with other techniques such as quantization and batch mixing. Moreover, we have shown that slowly increasing ϵ_{train} does not avoid poor local minima in MNIST. Similarly, [9] use the convergence score as a metric to imitate a curriculum. We show that there is a correlation between the convergence score and our probability gap, but our scheme is more closely related to the formal definition of curriculum learning and yield a more significant improvement over AT.

6 Conclusion

In this work, we have proposed ATES, a simple form of curriculum learning on AT using the softmax probability gap as a difficulty metric, which can be shown empirically related to the ideal metric. Our approach addresses the problems of AT where insufficiently large models can get stuck in poor local minima and achieve low clean accuracy. On larger models and datasets, ATES-S still shows a significant improvement over AT, consistently achieving higher clean and adversarial accuracy for all range of ϵ_{train} . A formal explanation of how curriculum learning with a well-defined difficulty metric helps avoid poor local minima and improves generalization is left for future work.

Acknowledgement

Part of the work done at IBM research was sponsored by the Combat Capabilities Development Command Army Research Laboratory and was accomplished under Cooperative Agreement Number W911NF-13-2-0045 (ARL Cyber Security CRA). The views and conclusions contained in this document are those of the authors and should not be interpreted as representing the official policies, either expressed or implied, of the Combat Capabilities Development Command Army Research Laboratory or the U.S. Government. The U.S. Government is authorized to reproduce and distribute reprints for Government purposes not withstanding any copyright notation here on.

The work done at UC Berkeley was supported by the Hewlett Foundation through the Center for Long-Term Cybersecurity and by generous gifts from Huawei, Google, and the Berkeley Deep Drive project.

References

- [1] Battista Biggio, Igino Corona, Davide Maiorca, Blaine Nelson, Nedim Šrndić, Pavel Laskov, Giorgio Giacinto, and Fabio Roli. Evasion attacks against machine learning at test time. In Hendrik Blockeel, Kristian Kersting, Siegfried Nijssen, and Filip Železný, editors, *Machine Learning and Knowledge Discovery in Databases*, pages 387–402, Berlin, Heidelberg, 2013. Springer Berlin Heidelberg.
- [2] Christian Szegedy, Wojciech Zaremba, Ilya Sutskever, Joan Bruna, Dumitru Erhan, Ian J. Goodfellow, and Rob Fergus. Intriguing properties of neural networks. *CoRR*, abs/1312.6199, 2013.
- [3] Ian J Goodfellow, Jonathon Shlens, and Christian Szegedy. Explaining and harnessing adversarial examples. In *International Conference on Learning Representations*, 2015.

- [4] Anish Athalye, Nicholas Carlini, and David A. Wagner. Obfuscated gradients give a false sense of security: Circumventing defenses to adversarial examples. *CoRR*, abs/1802.00420, 2018.
- [5] Aleksander Madry, Aleksandar Makelov, Ludwig Schmidt, Dimitris Tsipras, and Adrian Vladu. Towards deep learning models resistant to adversarial attacks. *CoRR*, abs/1706.06083, 2017.
- [6] Dimitris Tsipras, Shibani Santurkar, Logan Engstrom, Alexander Turner, and Aleksander Madry. Robustness may be at odds with accuracy. In *International Conference on Learning Representations*, 2019.
- [7] Yoshua Bengio, Jérôme Louradour, Ronan Collobert, and Jason Weston. Curriculum learning. In *Proceedings of the 26th Annual International Conference on Machine Learning*, ICML '09, page 41–48, New York, NY, USA, 2009. Association for Computing Machinery.
- [8] Yogesh Balaji, Tom Goldstein, and Judy Hoffman. Instance adaptive adversarial training: Improved accuracy tradeoffs in neural nets. *ArXiv*, abs/1910.08051, 2019.
- [9] Yisen Wang, Xingjun Ma, James Bailey, Jinfeng Yi, Bowen Zhou, and Quanquan Gu. On the convergence and robustness of adversarial training. In Kamalika Chaudhuri and Ruslan Salakhutdinov, editors, *Proceedings of the 36th International Conference on Machine Learning*, volume 97 of *Proceedings of Machine Learning Research*, pages 6586–6595, Long Beach, California, USA, 09–15 Jun 2019. PMLR.
- [10] Florian Schroff, Dmitry Kalenichenko, and James Philbin. Facenet: A unified embedding for face recognition and clustering. In *The IEEE Conference on Computer Vision and Pattern Recognition (CVPR)*, June 2015.
- [11] R. G. Cinbis, J. Verbeek, and C. Schmid. Weakly supervised object localization with multi-fold multiple instance learning. *IEEE Transactions on Pattern Analysis and Machine Intelligence*, 39(1):189–203, Jan 2017.
- [12] Junhyuk Oh, Xiaoxiao Guo, Honglak Lee, Richard L Lewis, and Satinder Singh. Action-conditional video prediction using deep networks in atari games. In C. Cortes, N. D. Lawrence, D. D. Lee, M. Sugiyama, and R. Garnett, editors, *Advances in Neural Information Processing Systems 28*, pages 2863–2871. Curran Associates, Inc., 2015.
- [13] Dario Amodei, Sundaram Ananthanarayanan, Rishita Anubhai, Jingliang Bai, Eric Battenberg, Carl Case, Jared Casper, Bryan Catanzaro, Qiang Cheng, Guoliang Chen, Jie Chen, Jingdong Chen, Zhijie Chen, Mike Chrzanowski, Adam Coates, Greg Diamos, Ke Ding, Niandong Du, Erich Elsen, Jesse Engel, Weiwei Fang, Linxi Fan, Christopher Fougner, Liang Gao, Caixia Gong, Awni Hannun, Tony Han, Lappi Johannes, Bing Jiang, Cai Ju, Billy Jun, Patrick LeGresley, Libby Lin, Junjie Liu, Yang Liu, Weigao Li, Xiangang Li, Dongpeng Ma, Sharan Narang, Andrew Ng, Sherjil Ozair, Yiping Peng, Ryan Prenger, Sheng Qian, Zongfeng Quan, Jonathan Raiman, Vinay Rao, Sanjeev Satheesh, David Seetapun, Shubho Sengupta, Kavya Srinet, Anuroop Sriram, Haiyuan Tang, Liliang Tang, Chong Wang, Jidong Wang, Kaifu Wang, Yi Wang, Zhijian Wang, Zhiqian Wang, Shuang Wu, Likai Wei, Bo Xiao, Wen Xie, Yan Xie, Dani Yogatama, Bin Yuan, Jun Zhan, and Zhenyao Zhu. Deep speech 2 : End-to-end speech recognition in english and mandarin. In Maria Florina Balcan and Kilian Q. Weinberger, editors, *Proceedings of The 33rd International Conference on Machine Learning*, volume 48 of *Proceedings of Machine Learning Research*, pages 173–182, New York, New York, USA, 20–22 Jun 2016. PMLR.
- [14] Joseph Turian, Lev Ratinov, and Yoshua Bengio. Word representations: A simple and general method for semi-supervised learning. In *Proceedings of the 48th Annual Meeting of the Association for Computational Linguistics*, ACL '10, page 384–394, USA, 2010. Association for Computational Linguistics.
- [15] K. Arulkumaran, M. P. Deisenroth, M. Brundage, and A. A. Bharath. Deep reinforcement learning: A brief survey. *IEEE Signal Processing Magazine*, 34(6):26–38, Nov 2017.
- [16] Jayesh K. Gupta, Maxim Egorov, and Mykel Kochenderfer. Cooperative multi-agent control using deep reinforcement learning. In Gita Sukthankar and Juan A. Rodriguez-Aguilar, editors, *Autonomous Agents and Multiagent Systems*, pages 66–83, Cham, 2017. Springer International Publishing.
- [17] Daphna Weinshall, Dan Amir, and Gad Cohen. Curriculum learning by transfer learning: Theory and experiments with deep networks. *CoRR*, abs/1802.03796, 2018.

- [18] Leslie N. Smith. Cyclical learning rates for training neural networks. *2017 IEEE Winter Conference on Applications of Computer Vision (WACV)*, pages 464–472, 2015.
- [19] Leslie N. Smith and Nicholay Topin. Super-convergence: Very fast training of residual networks using large learning rates. *CoRR*, abs/1708.07120, 2017.
- [20] Eric Wong, Leslie Rice, and J. Zico Kolter. Fast is better than free: Revisiting adversarial training. In *International Conference on Learning Representations*, 2020.
- [21] Kaiming He, Xiangyu Zhang, Shaoqing Ren, and Jian Sun. Identity mappings in deep residual networks. *CoRR*, abs/1603.05027, 2016.
- [22] Sergey Zagoruyko and Nikos Komodakis. Wide residual networks. *ArXiv*, abs/1605.07146, 2016.
- [23] Minhao Cheng, Simranjit Singh, Patrick H. Chen, Pin-Yu Chen, Sijia Liu, and Cho-Jui Hsieh. Sign-opt: A query-efficient hard-label adversarial attack. In *International Conference on Learning Representations*, 2020.
- [24] Wieland Brendel, Jonas Rauber, Matthias Kümmeler, Ivan Ustyuzhaninov, and Matthias Bethge. Accurate, reliable and fast robustness evaluation. In *NeurIPS*, 2019.
- [25] Hongyang Zhang, Yaodong Yu, Jiantao Jiao, Eric P. Xing, Laurent El Ghaoui, and Michael I. Jordan. Theoretically principled trade-off between robustness and accuracy. *CoRR*, abs/1901.08573, 2019.
- [26] Gavin Weiguang Ding, Yash Sharma, Kry Yik Chau Lui, and Ruitong Huang. Mma training: Direct input space margin maximization through adversarial training. In *International Conference on Learning Representations*, 2020.
- [27] Yisen Wang, Difan Zou, Jinfeng Yi, James Bailey, Xingjun Ma, and Quanquan Gu. Improving adversarial robustness requires revisiting misclassified examples. In *International Conference on Learning Representations*, 2020.
- [28] Minhao Cheng, Qi Lei, Pin-Yu Chen, Inderjit S. Dhillon, and Cho-Jui Hsieh. Cat: Customized adversarial training for improved robustness. *CoRR*, abs/2002.06789, 2020.
- [29] Qi-Zhi Cai, Min Du, Chang Liu, and Dawn Xiaodong Song. Curriculum adversarial training. In *IJCAI*, 2018.

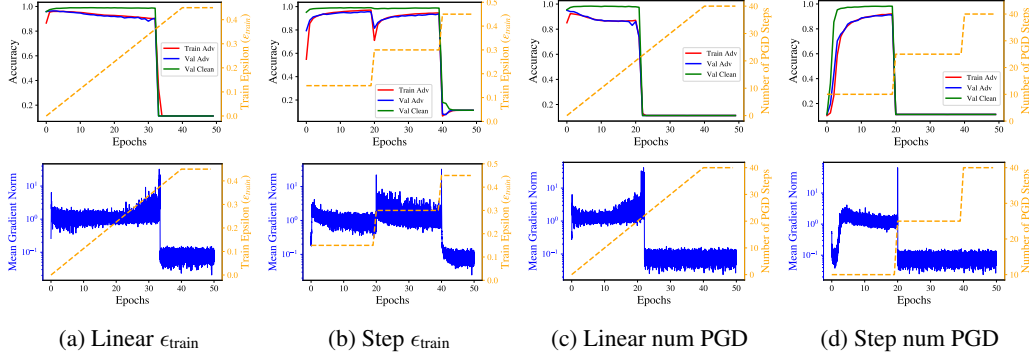


Figure 9: Experiments with combinations of two naive difficulty metrics (ϵ_{train} and the number of PGD steps) and two schedules (Linear and Step). The right axis (orange) of every plot shows values of the corresponding metric at each epoch. The top row shows the train adversarial accuracy (red), the validation adversarial (blue) and clean (green) accuracy. The bottom row shows gradient norms with respect to weights at every iteration or minibatch.

A Detailed Description of the Neural Networks

The neural networks we experiment with all use ReLU as the activation function and are trained using SGD with momentum of 0.9, batch size of 128, and weight decay of 5×10^{-4} except for the WideResNet model which uses a decay of 2×10^{-4} . We use early stopping during training (not related to ATES), i.e. we evaluate the models at the end of each epoch and only save ones with the highest adversarial validation accuracy seen so far.

Dataset-specific details of the training as well as brief descriptions of the model architecture are provided below.

MNIST. All experiments use the same three-layer convolution network. Models are trained for 70 epochs. The initial learning rate is set at 0.01 and is decreased by a factor of 10 at epochs 40, 50, and 60. During training, we run PGD for 40 steps with a step size of 0.02 and use a uniform random initialization within the ℓ_∞ -ball of radius ϵ_{train} for both AT and ATES.

CIFAR-10/CIFAR-100. We use both pre-activation ResNet-20 [21] and WideResNet-34-10 [22], which are trained for 100 epochs. Both AT and ATES use PGD with 10 steps and random restart. For $\epsilon_{\text{train}} < 16/255$, we use an initial learning rate of 0.1 and PGD step size of $2/255$. Otherwise, the initial learning is reduced to 0.01 with PGD step size of $4/255$. Standard data augmentation (random crop, flip, scaling, and brightness jitter) is also used.

B Choosing The Right Difficulty Metric

We begin by reiterating the connection between adversarial strength and the difficulty of the generated adversarial examples. We call an adversary “weak” when it generates “easy” adversarial examples, and similarly call an adversary “strong” when it generates “difficult” to accurately classify adversarial examples. To define the “difficulty” of a generated adversarial example, we experimented with a number of simple and intuitive choices for difficulty metrics before settling on the softmax probability gap. Two such simple metrics to control the strength of an adversary are: (i) ϵ_{train} , and (ii) the number of PGD steps, such that smaller the value of the metric weaker the adversary and vice versa. To increase the difficulty level of the adversarial examples, we increased the value of these metrics until they reached the desired final values (e.g., for MNIST, these values are $\epsilon_{\text{train}} = 0.45$ with 40 PGD steps). Note, scheduling ϵ_{train} to generate a curriculum is not a new idea and it has already been experimented with in [29].

We attempt to control these metrics using two different schedules: (i) Linear (increase the metric linearly with epoch until plateau at epoch 40), and (ii) Step (increase the metric in steps at epoch 20 and 40). When one metric is varied, the other stays fixed at the final desired value (i.e., when we schedule ϵ_{train} , the number of PGD steps is fixed at 40, throughout training). Figure 9 shows various accuracy curves (train adversarial accuracy, validation adversarial accuracy, and clean accuracy) of

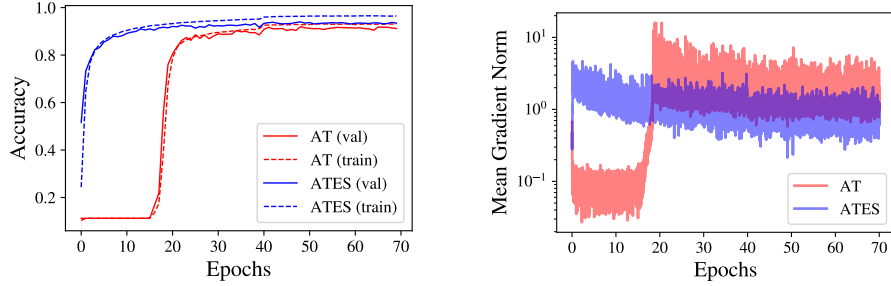


Figure 10: Comparison of accuracy (left) and gradient norm (right) during training of AT (red) and ATES (blue) on MNIST with $\epsilon_{\text{train}} = 0.3$.

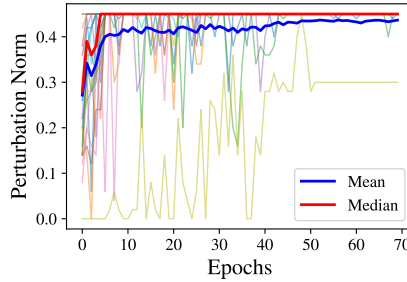


Figure 11: The actual perturbation norm of the adversarial examples generated by ATES on MNIST training set for $\epsilon_{\text{train}} = 0.45$. Note that we do not use a random start here as it would initially add a large perturbation and make the trend much more obscure. If the a smaller learning rate is used, the increase in the norms should be at a slower pace.

models trained using a combination of the two metrics under the two schedules. All models get stuck and admit a trivial solution after a certain number of epochs as their corresponding metric exceeds some thresholds. This demonstrates that the two naive metrics (ϵ_{train} and number of PGD steps) are insufficient for controlling the difficulty of adversarial examples.

Controlling Gradient Norms: Furthermore, corresponding to the epoch where the models abruptly turns into a constant function (both clean and adversarial accuracy drop to around 10%), the gradient norm with respect to the weights (Figure 9: bottom row) also shoots up for at least about an order of magnitude. This leads us to suspect that the extremely large gradient update gets the model into a poor local minima. Finally, gradient norm can be controlled directly via the loss which can in-turn be controlled by the softmax probability – motivating our difficult metric.

To show that ATES does affects gradient norms, we train two models with $\epsilon_{\text{train}} = 0.3$ using AT and ATES. Figure 10 confirms our intuition. On one hand, ATES helps avoid large jumps in gradient norm and also decreases the overall norm. On the other hand, the AT model starts off slow and seems to get stuck in a local minima. However, after around 20 epochs, the AT model escapes the local minima as the gradient norm jumps up significantly together with the accuracy.

B.1 Relationship between our metric and perturbation norm

Even though using ϵ_{train} as a difficulty metric directly fails to solve the issue on MNIST, we argue that there is a relationship between this metric and ours. As we have previously mentioned in Section 3.2 in the main text, our intuition is that as training progresses, the decision boundary gets pushed away from each sample which slowly increases the average distance between training samples and the boundary. We empirically verify this statement by training networks using ATES on MNIST with $\epsilon_{\text{train}} = 0.45$ and CIFAR-10 with $\epsilon_{\text{train}} = 16/255$ and keeping track of the true perturbation norm of 20 training samples across all epochs. Figure 11 and 12 plot the norms as well as their average. As expected, the perturbation norms of most samples start small and significantly increase after a few epoch.

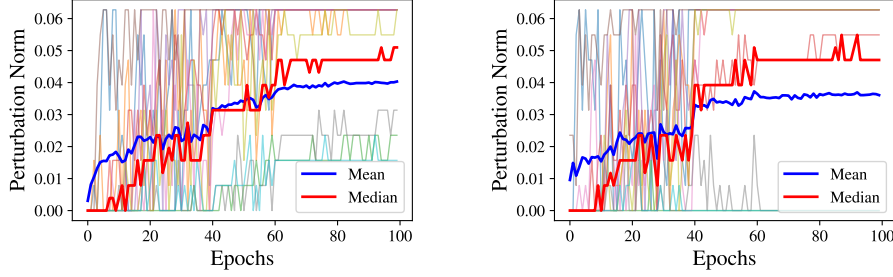


Figure 12: The actual perturbation norm of the adversarial examples generated by ATES (left) and ATES-S (right) on CIFAR-10 training set for $\epsilon_{\text{train}} = 16/255$. We also do not use a random start here.

Note, the increase in the perturbation norms is not linear. Some fluctuations are also observed, but on average, the boundary is progressively moved further away from the training samples. The complex relationship between the norms and the training epochs as well as the fluctuation suggests why naively increasing ϵ_{train} as a linear or step function of epochs does not work as well as our method.

Additionally, we can observe that the perturbation norm increases at a faster rate for ATES-S compared to ATES. Especially, there is a large jump at epoch 40 for ATES-S because it is the first epoch that the probability gap is increased to 0.333. When the gap becomes larger, the PGD can terminate later which increases the perturbation norm.

C Evaluating Adversarial Robustness Using PGD+

We measure the adversarial robustness of a model at a given ϵ_{test} as the model’s accuracy given that all of its input can be perturbed using a noise budget of size at most ϵ_{test} . However, adversarial robustness is notoriously difficult to evaluate empirically. Therefore, we take special care to ensure that as many adversarial examples as possible are found for a given perturbation budget.

Towards this end, we extend PGD (standard attack for ℓ_∞ -norm perturbation) and call it PGD+. It consists of 30 PGD runs for MNIST and 20 for CIFAR-10 with 100 steps each. The runs compose of

1. Five random restarts initialized around a given test sample.
2. Five random restarts initialized around the closest training sample that is classified by the model as one of the incorrect classes and projected back to the ℓ_∞ -ball around the test sample. This step is only used for MNIST but not CIFAR-10.
3. Five random restarts, each of which is initialized around one of the five nearest training samples. The initialized points are all projected back to the ℓ_∞ -ball constraint before starting a run.
4. All fifteen runs (1. - 3.) described above are repeated twice, one maximizing cross-entropy loss to generate attacks and another using hinge loss.

If any of the runs (30 for MNIST and 20 for CIFAR-10) result in a successful attack, we consider that the test sample has been misclassified at a given ϵ_{test} . Note, we focus on random initialization from different starting points. This is particularly important for non-convex optimization. Using two loss functions does not only increase the number of random restarts but also decreases the chance of two potential problems: Saturation of cross-entropy loss and slow convergence of hinge loss.

D Theoretical Results on Logistic Regression

In this section, we prove a theoretical result on a linear classifier.

Proposition 1. *ATES on logistic regression problem trained with gradient descent forms a curriculum according to the ideal difficulty metric.*

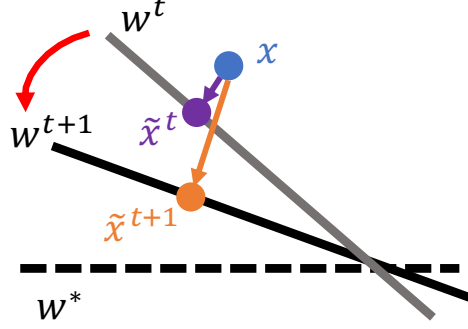


Figure 13: Adversarial example generated at iteration t , \tilde{x}^t , is further from the ideal boundary and hence, has lower loss than \tilde{x}^{t+1} .

Define (x, y) a pair of sample and its ground truth label which takes value 0 or 1. Denote the logistic classifier f parameterized by weight w , and logistic loss L . Assume that the weight $w \in \mathbb{R}^d$ is normalized, i.e. $\|w\|_2 = 1$. This makes no difference in term of 0-1 loss. We ignore the bias term for simplicity as it can always be subsumed by w . Let w^* denote the optimal weight or hypothesis for a given dataset.

$$f(x; w) := \sigma(\langle w, x \rangle) := \frac{1}{1 + e^{-\langle w, x \rangle}} \quad (6)$$

$$L(x, y; w) := -y \log(f(x; w)) - (1 - y) \log(1 - f(x; w)) \quad (7)$$

$$w^* := \arg \min_w \frac{1}{n} \sum_{i=1}^n \max_{\delta: \|\delta\| \leq \epsilon_{\text{train}}} L(x_i + \delta, y_i; w) \quad (8)$$

Finally, \tilde{x}^t denotes an adversarial example generated from x by ATES given the weight w^t of the classifier at iteration t . In other words, \tilde{x}^t is a projection of x onto the hyperplane $\{x \in \mathbb{R}^d \mid \langle w^t, x \rangle = 0\}$. Our early stopping technique approximates this projection. The smaller the step size of PGD, the better the approximation.

$$\tilde{x}^t = \text{proj}_{w^t}(x) \quad (9)$$

Now Proposition 1 can be translated to:

$$L(\tilde{x}^t, y; w^*) \leq L(\tilde{x}^{t+1}, y; w^*) \quad (10)$$

We will prove Proposition 1 first under ℓ_2 -norm adversary and then ℓ_∞ -norm adversary. Consider a training sample x with label 1 that is correctly classified at iteration t , i.e. $f(x; w^t) \geq \frac{1}{2}$. The case where x is misclassified is trivial as it will not be perturbed and so $L(\tilde{x}^t, y; w^*) = L(\tilde{x}^{t+1}, y; w^*) = L(x, y; w^*)$.

D.1 ℓ_2 -norm adversary

First, we state our Claim 1:

$$\langle w^t, w^* \rangle \leq \langle w^{t+1}, w^* \rangle \quad (11)$$

Proof. This can be shown by the descent condition of gradient descent on convex function. Since logistic loss is convex, its robust version which is a point-wise maximum (over δ) of a set of convex functions is also convex. Hence, it is true that

$$\|w^t - w^*\|_2^2 \geq \|w^{t+1} - w^*\|_2^2 \quad (12)$$

$$\|w^t\|_2^2 + \|w^*\|_2^2 - 2\langle w^t, w^* \rangle \geq \|w^{t+1}\|_2^2 + \|w^*\|_2^2 - 2\langle w^{t+1}, w^* \rangle \quad (13)$$

$$\langle w^t, w^* \rangle \leq \langle w^{t+1}, w^* \rangle \quad (\|w\|_2 = 1) \quad (14)$$

□

In this case, we can write \tilde{x}^t explicitly as

$$\tilde{x}^t = \text{proj}_{w^t}(x) = x - \frac{\langle w^t, x \rangle}{\|w^t\|_2^2} w^t = x - \langle w^t, x \rangle w^t \quad (15)$$

Then we take inner product on both sides with w^* :

$$\langle w^*, \tilde{x}^t \rangle = \langle w^*, x \rangle - \langle w^t, x \rangle \langle w^*, w^t \rangle \quad (16)$$

$$\geq \langle w^*, x \rangle - \langle w^{t+1}, x \rangle \langle w^*, w^t \rangle \quad (\text{Condition on } x) \quad (17)$$

$$\geq \langle w^*, x \rangle - \langle w^{t+1}, x \rangle \langle w^*, w^{t+1} \rangle \quad (\text{Claim 1}) \quad (18)$$

$$= \langle w^*, \tilde{x}^{t+1} \rangle \quad (19)$$

$$\Rightarrow f(\tilde{x}^t; w^*) \geq f(\tilde{x}^{t+1}; w^*) \quad (20)$$

$$\Rightarrow L(\tilde{x}^t, y; w^*) \leq L(\tilde{x}^{t+1}, y; w^*) \quad (21)$$

From line (11) to (12), we use the condition on x that

$$\langle w^t, x \rangle \leq \langle w^{t+1}, x \rangle \quad (22)$$

To put differently, every x that satisfies this condition at any iteration t will follow a curriculum under the ideal difficulty metric. This condition is true on average but cannot be guaranteed for any x . It is equivalent to a statement that the distance from x to the boundary is increased in the next iteration. Figure 13 gives a geometric interpretation of this proof.

D.2 ℓ_∞ -norm adversary

Similarly, we write \tilde{x}^t as a projection of x onto a hyperplane $\{x \in \mathbb{R}^d \mid \langle w^t, x \rangle = 0\}$ but now in ℓ_∞ -distance. The closed form of \tilde{x}^t can be written as follows

$$\tilde{x}_j^t = x_j + \frac{|\langle w^t, x \rangle|}{\|w^t\|_1} \cdot \text{sgn} \left(\frac{-\langle w^t, x \rangle}{w_j^t} \right) \quad (23)$$

The ℓ_∞ -distance from x to the hyperplane w^t or the norm of this perturbation is then $d(w^t, x) := \frac{|\langle w^t, x \rangle|}{\|w^t\|_1}$. Next the proof goes analogously to the ℓ_2 case. We take an inner product with w^* on both sides.

$$\langle w^*, \tilde{x}^t \rangle = \langle w^*, x \rangle + \frac{|\langle w^t, x \rangle|}{\|w^t\|_1} \left(\sum_{j=1}^d \text{sgn} \left(\frac{-\langle w^t, x \rangle}{w_j^t} \right) w_j^* \right) \quad (24)$$

$$= \langle w^*, x \rangle + \frac{|\langle w^t, x \rangle|}{\|w^t\|_1} \left(\sum_{j=1}^d \text{sgn}(-w_j^t w_j^*) \right) \quad (25)$$

The last line comes from that fact that we specify x to be correctly classified by w^t so $\langle w^t, x \rangle \geq 0$. The first term on the RHS is fixed so we can ignore it. Now we make another assumption (Assumption 1):

$$\sum_{j=1}^d \text{sgn}(-w_j^t w_j^*) \leq 0 \quad (26)$$

This assumption is easy to satisfy. It says that w^t and w^* have more elements with the same sign than not. If w^0 is randomly initialized, the signs are already matched half the times from the beginning, and any subsequent updates should align more of them. This is also true when w^0 is initialized at 0. Taking Assumption 1, we can simplify equation 25 as follows:

$$\langle w^*, \tilde{x}^t \rangle = \langle w^*, x \rangle - C \frac{|\langle w^t, x \rangle|}{\|w^t\|_1} \quad (\text{for some } C \geq 0) \quad (27)$$

$$\geq \langle w^*, x \rangle - C \frac{|\langle w^{t+1}, x \rangle|}{\|w^{t+1}\|_1} \quad (\text{Condition on } x) \quad (28)$$

$$= \langle w^*, \tilde{x}^{t+1} \rangle \quad (29)$$

$$\Rightarrow f(\tilde{x}^t; w^*) \geq f(\tilde{x}^{t+1}; w^*) \quad (30)$$

$$\Rightarrow L(\tilde{x}^t, y; w^*) \leq L(\tilde{x}^{t+1}, y; w^*) \quad (31)$$

This concludes the proof. The condition on x is similar to its ℓ_2 counterpart:

$$\frac{|\langle w^t, x \rangle|}{\|w^t\|_1} \leq \frac{|\langle w^{t+1}, x \rangle|}{\|w^{t+1}\|_1} \quad (32)$$

This quantity is the shortest distance in ℓ_∞ -norm from x to the hyperplane $\langle w, x \rangle = 0$. So this assumption corresponds to “after taking one weight update, the decision boundary is the same distance or now further from x in ℓ_∞ -norm.”